

Available online at www.sciencedirect.com



Scripta Materialia 50 (2004) 483-487



www.actamat-journals.com

Effect of T-stress on dislocation emission in iron

Glenn E. Beltz a,*, Anna Machová b

a Department of Mechanical Engineering, University of California, Santa Barbara, CA 93106-5070, USA
 b Institute of Thermomechanics, Academy of Sciences of the Czech Republic, Dolejskova 5, 18200 Prague 8, Czech Republic
 Received 10 September 2003; received in revised form 25 October 2003; accepted 28 October 2003

Abstract

We compare continuum predictions for dislocation emission from a crack tip loaded under mode I, biaxial conditions with atomistic results for bcc iron. The simulations validate the continuum prediction that, as the *T*-stress increases, so does the threshold for dislocation nucleation; hence, the propensity for brittle response increases.

© 2003 Acta Materialia Inc. Published by Elsevier Ltd. All rights reserved.

Keywords: Atomistic simulation; Dislocation nucleation; Fracture; T-stress; Iron

1. Introduction

Atomistic situations, such as those based on the molecular dynamic technique (MD), offer an opportunity to study the brittle vs. ductile behavior independently of empirical failure criteria oft-times associated with continuum models. The only failure criterion used in MD simulations is the cut-off radius of nonlinear interatomic forces. As specific examples, the generation of defects (e.g., microcracks, dislocations, twins) or crack tip blunting can be studied with MD simulations and are seen as spontaneous processes controlled solely by the interatomic forces and external conditions. Unlike continuum elastic models, atomistic simulations avoid stress singularities that are associated with crack tips and dislocation cores, and enable the validation or further development of failure criteria used in continuum models. The present contribution represents an effort to overcome existing contradictions between atomistic results, e.g. [1], and the ductile vs. brittle prediction by Rice [2] based on the Peierls-Nabarro dislocation model.

Specifically, we compare MD results on the ductile vs. brittle response of bcc iron under biaxial loading and plane strain conditions with a recent continuum model by Beltz and Fischer [3] that incorporates the *T*-stress

E-mail address: beltz@engineering.ucsb.edu (G.E. Beltz).

(discussed in further detail below) into Rice's model. Our findings show a reasonable consistency between the continuum and atomistic results, but, more importantly, represent the first time that the *T*-stress has been systematically controlled in an atomistic simulation to influence crack stability.

The details of the stress state around a crack tip in an elastic solid are often characterized by a single parameter, the stress intensity factor K that expresses the strength of the singularity as the crack tip is approached. This parameter has proven extremely useful for quantifying when a crack might begin to propagate, or when it might emit a dislocation (or other shear-like feature) and subsequently blunt. It has long been recognized that a nonsingular contribution to the stress field (that is, a term that remains finite as the crack tip is approached, also known as the "T-stress") may have some effect on the stability of a propagating crack. However, the effects of including the T-stress in models for dislocation nucleation have largely been ignored. Beltz and Fischer [3] recently incorporated this term into the Rice model [2] for dislocation nucleation at a crack tip in an isotropic medium. It was found that, in addition to the unstable stacking energy γ_{us} (introduced in [2] from block-like shear displacement of a crystal), the T-stress is also important and has a modest impact on the brittle-ductile behavior of short cracks. This paper demonstrates the importance of the *T*-stress in atomistic simulations. The T-stress can decrease the applied load needed for dislocation emission, and hence it is incumbent to properly account for it when attempting to reconcile

^{*}Corresponding author. Tel.: +1-805-893-3354; fax: +1-805-893-8651

atomistic simulations with continuum-based predictions (e.g., Refs. [1,4–6]).

An important consideration in this undertaking is the relative orientation of the crack plane and available slip system(s). Specifically, if the active slip system in bcc iron is considered to be $\langle 111 \rangle \{112\}$, then generally three different shear processes may be observed at a crack tip under plane strain conditions: (i) generation of unstable stacking faults, (ii) twinning, or (iii) emission of edge dislocations. Molecular dynamic simulations (MD) in bcc iron [7,8] have shown that, for the crack orientation (001)[110] (crack plane/crack front), generation of unstable stacking faults and twinning at the crack tip are preferred on the $\langle 1 \ 1 \ 1 \rangle \langle 1 \ 1 \ 2 \rangle$ slip systems; while, for the crack orientation $(\bar{1} \ 1 \ 0)[1 \ 1 \ 0]$, emission of complete edge dislocations is observed on the same type of slip system [9]. This can be explained by the fact that the active shear systems ($\langle 111 \rangle \langle 112 \rangle$) ahead of the crack tip are oriented in the easy twinning direction for the crack (001)[110] and in the hard (or "anti-twinning") direction for the crack (110)[110]. In this paper, we focus on the latter orientation, that is, the one associated with dislocation nucleation.

2. Preliminaries

Following the work of Williams [10], the asymptotic representation of the stress field in the vicinity of a crack, ignoring terms of $r^{1/2}$ and higher, can be expressed as

$$\begin{bmatrix} \sigma_{11} & \sigma_{12} \\ \sigma_{21} & \sigma_{22} \end{bmatrix} = \frac{K}{\sqrt{2\pi r}} \begin{bmatrix} S_{11}(\theta) & S_{12}(\theta) \\ S_{21}(\theta) & S_{22}(\theta) \end{bmatrix} + \begin{bmatrix} T & 0 \\ 0 & 0 \end{bmatrix}, \quad (1)$$

where K is the well-known "applied" stress intensity factor, the terms $S_{ij}(\theta)$ give the angular variation of the field (which may be found for a generally anisotropic solid in Ref. [11]), and T is independent of θ . For a central crack of length 2a in an infinite domain subject to remote tension σ_A perpendicular to the crack and σ_B parallel to the crack (Fig. 1), K and T are given by

 $\sigma_{\rm A}\sqrt{\pi a}$ and $\sigma_{\rm B}+{\rm Re}[\mu_1\mu_2]\sigma_{\rm A}$, respectively [12]. The parameters μ_1 and μ_2 are roots of a characteristic equation formed by the anisotropic constants [11,12], and reduce to $\sqrt{-1}$ for an isotropic solid. In this paper, we consider only *proportional* loading histories, that is, the ratio $\sigma_{\rm B}/\sigma_{\rm A}$ (hereafter referred to as α) is held at a prescribed value as the cracked system is loaded. Thus, the *T*-stress may be expressed in terms of the stress intensity factor

$$T = \frac{K[\alpha + \text{Re}(\mu_1 \mu_2)]}{\sqrt{\pi a}} \tag{2}$$

and it is seen that the relative magnitudes of K and T are interrelated to the crack size. In fact, Eq. (2) suggests there is a crack size effect, i.e., the effect of T-stress should diminish as crack size increases.

3. MD simulations

The MD simulations described in this section use an N-body potential of the Finnis-Sinclair type [7,8], applied to an iron crystal at 0 K under plane strain. The potential is consistent with the elastic constants $C_{11} = 2.433$, $C_{12} = 1.45$, and $C_{44} = 1.16 \times 10^{11}$ Pa. We consider a pre-existing atomically sharp central crack of the length 2a embedded in an initially rectangular sample. The crack surfaces lie on (110) planes, the crack front is oriented along the [110] direction, and crack extension, if it were to occur, would be in the [001] direction. The crack is loaded in mode I, i.e., a uniform traction σ_A perpendicular to the crack is applied along the top and bottom boundaries; additionally, we consider biaxial loading by adding a far field stress $\sigma_{\rm B}$ parallel to the crack plane. Due to the symmetry of the problem, we only simulate one half of the sample in the x_1 -direction, with half crack length a. Thus, atoms lying at the left border of the sample are constrained to move only in the x_2 -direction. The sample consists of 300 planes both in the x_1 and x_2 directions. The initial crack size is given by $a = 15a_0$, where $a_0 = 2.8665$ Å is the lattice parameter.

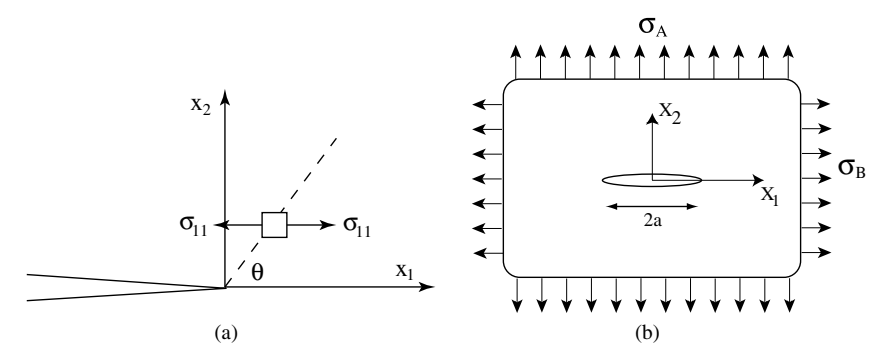


Fig. 1. (a) Schematic of crack and slip plane (dashed) inclined at angle θ . The T-stress gives a contribution to σ_{11} in addition to the classical K-field result. (b) Finite crack of length 2a in a solid, with remotely applied stresses σ_A and σ_B .

Prior to the external loading, the samples are relaxed to avoid the influence of surface relaxation on crack tip processes. The Newtonian equations of motion for individual atoms are solved by the central difference method using time integration steps of magnitude 10^{-14} s. Thermal atomic motion is not controlled in the system: That is, atomic velocities are not prescribed as in Refs. [7–9]. The global energy balance

$$W_{\text{ext}}(t) = E_{\text{pot}}(t,0) + E_{\text{kin}}(t) \tag{3}$$

in the assemblage is monitored at each time step. Here, $W_{\rm ext}(t)$ denotes the work done by the external forces, $E_{\rm pot}(t,0)=E_{\rm pot}(t)-E_{\rm pot}(0)$ is the change of the total potential energy during loading, and $E_{\rm kin}(t)$ is the total kinetic energy. We use a quasi-static loading, i.e., the total kinetic energy in the system is very low, as in earlier work [7].

3.1. Uniaxial loading

The sample is loaded up gradually to a level σ_A during 6000 time steps. When the prescribed stress level is reached, the applied stress is held constant (as in Fig. 3 in [7]). Dislocation emission is observed below the Griffith level $\sigma_G = K_G/\sqrt{\pi a}$, where K_G is the critical stress intensity factor given by the relation $2\gamma_s = CK_G^2$. Here $2\gamma_s$ is the work of decohesion and C is the appropriate anisotropic constant. We note that the relative crack/sample dimensions are sufficiently large that boundary correction procedures are not necessary [13].

No dislocation emission was observed in the simulation at a constant level of applied stress $\sigma_A = 6.48$ GPa. At the level $\sigma_A = 6.82$ GPa, dislocation emission was observed with a certain delay. At the level $\sigma_A = 7.16$ GPa, dislocation emission occurred at time step 6132, i.e., shortly after that stress level was reached. We thus observe "spontaneous" dislocation emission at an applied stress intensity K = 0.8134-0.8541 MPa m^{1/2}, a significantly lower value than $K_{\text{disl}} = 1.44 \text{ MPa} \,\text{m}^{1/2}$ from the Rice model that includes normal relaxation effects [4]. A preliminary study of the influence of Tstress in the Rice model has been examined by Beltz and Fischer [3]. They showed that the threshold for dislocation emission is reduced by about 25% for a crack of size $a/b \approx 17.32$. A more precise analysis of this effect will be given in Section 4.

3.2. Proportional biaxial loading

For a biaxiality ratio $\alpha = 1$ (that is, $T \approx 0$ in accordance with Eq. (2)), brittle crack initiation was observed in the MD simulation at time step 7513. The crack was initiated at applied stress intensity $K_{\rm A} \approx 0.93-0.99$ MPa m^{1/2} (the first value is corrected in consideration of the flight time of loading waves from the sample borders to the x_1 -axis). The work done by the normal stresses at

the crack tip at the initiation of fracture corresponds to a value 3.86 J/m^2 , close to the theoretical work of decohesion $2\gamma_s = 3.603 \text{ J/m}^2$, obtained in a perfect crystal strained axially in the $\langle 1\,1\,0\rangle$ directions under plane strain conditions. Using the anisotropic constant $C=3.868\times 10^{-12} \text{ m}^2/\text{N}$, the theoretical Griffith stress intensity factor is $K_G=0.965 \text{ MPa}\,\text{m}^{1/2}$, in good agreement with the MD results. For $\alpha>1$, we observe unstable crack extension.

For $\alpha=0.9$, significant bond breakage at the crack tip was observed in the simulation, but full crack initiation did not occur prior to the arrival of stress waves emitted from the crack tip and reflected back from external sample borders to the crack tip (expected at time step 8022). Nevertheless, the bond breakage indicates brittle behavior. For $\alpha=0.7$, some incipient dislocation activity and bond breakage at the crack tip were observed, but neither emission of a dislocation pair nor crack initiation were detected before time step 8000. Similar behavior was observed for $\alpha=0.65$.

For $\alpha=0.6$ and lower, the emission of complete pairs of dislocations was observed (as mentioned earlier, on the slip systems $\langle 1\,1\,1\rangle \{1\,1\,2\}$). Thus, we conclude that a transition takes place for ductile to brittle behavior for the $(\bar{1}\,1\,0)[1\,1\,0]$ crack as α increases through approximately 0.6–0.65. That is, for $\alpha>0.65$, brittle behavior at the crack tip is favored, while for $\alpha<0.65$, dislocation emission and crack tip blunting is favored.

4. Continuum predictions

We use the established Peierls framework for dislocation formation at a crack, which assumes that the dislocation/crack system can be thought of as two anisotropic elastic semi-spaces separated by a common plane (the crack plane and slip plane) on which there is a discontinuous jump in the displacement fields [2]. There exists a periodic relationship between shear stress and slip displacement along the slip plane, with traction-free surfaces along the crack plane. Prior to dislocation nucleation, there is a distribution of slip discontinuity along the slip plane that ultimately reaches a point of instability with increased applied load and results in the nucleation of a dislocation. Using this theory, a locus of *K* and *T* values at which nucleation occurs may be determined.

For all of the calculations presented here, a simple relationship due to Frenkel [14] between shear stress and slip displacement on the slip plane is assumed:

$$\tau(\delta) = \frac{\mu b}{2\pi h} \sin\left(\frac{2\pi\Delta}{b}\right) = \frac{\pi \gamma_{\rm us}}{b} \sin\left(\frac{2\pi\Delta}{b}\right),\tag{4}$$

where τ is the local shear stress ($\sigma_{r\theta}$ using the coordinates implied in Fig. 1), Δ is the relative atomic displacement between two atomic planes, h is the interplanar spacing

of those two planes, μ is the "effective" shear modulus for shear along the slip plane of interest (and can be written in terms of the anisotropic elastic constants), b is the Burgers vector, and γ_{us} is the unstable stacking energy (equal to $\mu b^2/2\pi^2 h$ in the Frenkel model). As introduced by Rice [2], the continuum analog to Δ (referred to as δ) is thought of as Δ extrapolated to a cut halfway between the slipping planes and is given by $\delta = \Delta - \tau h/\mu$. A shear softening process attributable to tensile forces across the slip plane can be a critical element in dislocation nucleation, as quantified by Sun et al. [4]. That analysis revealed that a reduced, or "effective," value of γ_{us} in Eq. (4) may be used to accurately characterize the slip plane response. We have neglected any consideration of tension-shear coupling in the current analysis for simplicity.

From elastic considerations, the stress along the slip plane can be written as

$$\tau[\delta(r)] = \frac{KS_{r\theta}(\theta)}{\sqrt{2\pi r}} - T\sin\theta\cos\theta$$
$$-\int_{0}^{\infty} g(r, s, \theta) \frac{\partial\delta(s)}{\partial s} ds, \tag{5}$$

where the first two terms on the right hand side give the pre-existing shear stress along the slip plane due to the applied load on the crack geometry (comprising the most singular term, scaled by K, as well as the constant term, proportional to T), and the third term reflects the stress relaxation that occurs due to sliding along the cut. The kernel g in the integral term represents the stress at distance r along the slip plane in an anisotropic solid due to a dislocation positioned at distance s, while $-(\partial \delta/\partial s) ds$ represents an infinitesimal Burgers vector (we exploit the notion that the slip distribution can be discretized into an array of infinitesimal dislocations). The first term on the right hand side of Eq. (5) is singular in r, but it is perfectly cancelled by an equal and opposite singularity in the third term; thus, the entire right hand side is bounded as $r \to 0$.

Eqs. (4) and (5) are seemingly incongruent, as (4) is nonlinear while (5) is based on linear elasticity. The problem addressed is best thought of as an externally loaded solid containing a crack with traction-free surfaces, with the additional boundary condition that the shear stress τ is a function of the slip displacement δ along a plane of discontinuity emanating from the crack tip. Thus, the nonlinearity is relegated to the boundary conditions of what otherwise is a linear problem.

We seek a slip distribution $\delta(r)$ such that, for all r > 0, $\tau[\delta(r)]$ predicted by the linear elastic formulation, Eq. (5), must equal $\tau[\delta]$ provided by the atomic-based shear relation in Eq. (4). Using a numerical procedure outlined by Beltz [15] and Beltz and Rice [16], we carry this out for incremental increases in K and T, which are linearly related to each other through Eq. (2), until an

instability (i.e., dislocation nucleation) is attained. The instability is said to occur when, for a given value of T, a maximum K is found for which a solution (in terms of a dislocation-like slip distribution) 1 can be found.

An alternate approach to solving Eq. (5) proceeds by recognizing that the grouping of terms $\tau[\delta(r)] + T\cos\theta\sin\theta$ acts as an "effective" stress vs. slip displacement law across the slip plane. The unstable stacking energy $\gamma_{\rm us}$ in any T=0 solution, such as available in Ref. [4], may be replaced by $\gamma_{\rm us} + Tb\cos\theta\sin\theta/2$ for an approximate solution. For the results generated in this paper, we have utilized a direct numerical procedure as outlined in the previous paragraph.

5. Results and discussion

Results from the continuum method are shown in Fig. 2, where the critical threshold for dislocation nucleation (expressed in terms of G, the energy release rate) is plotted as a function of biaxiality ratio α . The nominal range of values for our observed threshold exceeds $4\gamma_{us}$ (in seeming contradiction with the oft-cited result that $G \approx \gamma_{us}$ for dislocation nucleation), but this is due to the fact that the active slip plane is inclined at 54.7° with respect to the crack plane and thus the resolved shear stress acting on the plane is smaller for a given applied load.

Recall that $\alpha = 0$ gives a relatively large, negative Tstress, while $\alpha = 1$ corresponds to $T \approx 0$. We have not displayed results for large, positive T-stresses because, as mentioned earlier, they would increase the critical load for dislocation nucleation beyond the values found in this work and lead to brittle behavior. The general trend is that as the *T*-stress increases, so does the threshold for dislocation emission and the likelihood for the material to behave in a brittle manner. We note that the continuum method does not (directly) give a threshold for cleavage. That could simply be determined by the Griffith condition, that is, fracture would occur when $G = 2\gamma_s$, where the latter is associated with separating the $(\bar{1}10)$ plane in bcc iron. As indicated in the Fig. 2, the results from the continuum model are in qualitative agreement with those from the simulations. Further MD simulations, in larger assemblages, are needed to characterize the ductile-brittle transition more precisely.

It is of interest to compare the local kinetic and potential energies at the crack tip during dislocation emission in the MD simulations. At the critical point corresponding to dislocation nucleation or fracture, the

¹ Instability associated with a mode II, "crack-like" distribution of slip is not admissible in this model due to the nature of Eq. (4).

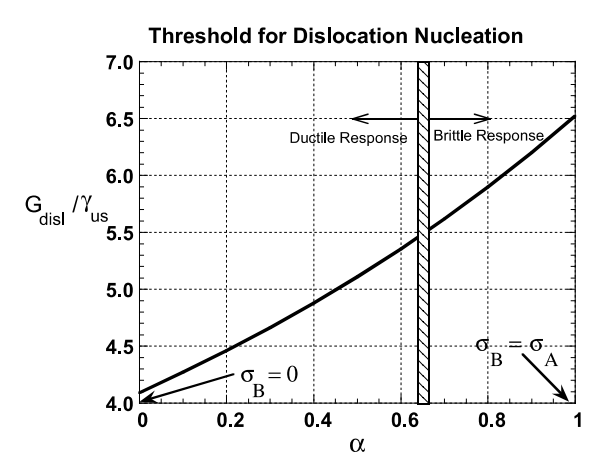


Fig. 2. Threshold for dislocation nucleation on a $\{211\}$ type plane from a $\{110\}$ crack in bcc iron at 0 K as a function of biaxiality ratio α (defined as the ratio σ_B/σ_A from Fig. 1b). For this crystal orientation, the angle θ (see Fig. 1) takes the value 54.7°.

local potential energy in the slip system reached the values of 1.06–1.245 J/m², while the local kinetic energy reached the negligible value 0.00112 J/m². After the critical point, the kinetic energy increased and the potential energy decreased. A smaller part of the released energy was absorbed via thermal atomic motion, while the larger part was transferred via stress waves emitted during the subsonic motion of dislocations (a further discussion of this aspect has been given by Landa et al. [9]).

The continuum prediction in Fig. 2 also improves significantly the agreement with the MD results for $\alpha=0$. Using the same constant C as above and the relaxed value of $\gamma_{\rm us}=1.06~{\rm J/m^2}$, the lowest stress intensity factor needed for dislocation emission from the updated model is 1.059 MPa m^{1/2}. It differs by only 16% from the upper limit $K_{\rm A}=0.889~{\rm MPa\,m^{1/2}}$ of the applied stress intensity in the simulation with $\alpha=0$. Such deviation from the elastic prediction can be explained by the nonlinear and dynamic phenomena at the crack tip in the simulations.

6. Conclusions

Our continuum predictions and atomistic simulations for bcc iron confirm the role of *T*-stress in ductile vs. brittle behavior of a crack tip. The reasonable agreement that we find is especially relevant for nano-cracks, where the *T* stress, if it is present, can significantly alter the distribution of stress from that given by linear elastic fracture mechanics based solely on the most singular term of the asymptotic stress expansion about a crack tip.

Acknowledgements

This research was supported by the National Science Foundation under award number CMS-0000142 and the Czech Science Foundation under grants A2076201, ME 504, and AV0Z2076919. We are grateful to Margherita Chang, Leah Ow, Carl Meinhart, and Don Lipkin for helpful discussions.

References

- [1] Shastry V, Farkas D. Model Simul Mater Sci Eng 1996;4:473.
- [2] Rice JR. J Mech Phys Solids 1992;46:239.
- [3] Beltz GE, Fischer LL. Multiscale deformation and fracture in materials and structures. Boston: Kluwer; 2001. p. 237.
- [4] Sun Y, Beltz GE, Rice JR. Mater Sci Eng A 1993;170:67.
- [5] Cleri F, Yip S, Wolf D, Phillpot SR. Phys Rev Lett 1997;79:1309.
- [6] Gumbsch P, Beltz GE. Model Simul Mater Sci Eng 1995;3:597.
- [7] Machová A, Beltz GE, Chang M. Model Simul Mater Sci Eng 1999;7:949.
- [8] Machová A, Ackland GJ. Model Simul Mater Sci Eng 1998;6:521.
- [9] Landa M, Cerv J, Machová A, Rosecky Z. J Acoustic Emission 2002;20:25.
- [10] Williams ML. J Appl Mech 1957;24:109.
- [11] Ting TCT. Anisotropic elasticity: theory and applications. New York: Oxford University Press; 1996.
- [12] Stroh AN. Phil Mag 1958;7:625.
- [13] Murakami Y. In: Stress intensity factor handbook, vol. 1. Oxford: Pergamon; 1987. p. 67.
- [14] Frenkel J. Zeitschrift f Physik 1926;37:572.
- [15] Beltz GE. The Mechanics of Dislocation Nucleation at a Crack Tip. PhD dissertation, Harvard University; 1992.
- [16] Beltz GE, Rice JR. Acta Metall Mater 1992;40:S321.